Controlling the electrochemical properties of spinel intercalation compounds

Sanjeev Krishna Kolli[†] and Anton Van der Ven[*,†,‡]

†*Materials Department, University of California Santa Barbara, Santa Barbara*

‡*Current address: 1361A Engineering II University of California, Santa Barbara,Santa Barbara, CA 93106-5050*

E-mail: avdv@ucsb.edu

Phone: +1(805)893-7920

Abstract

Spinel intercalation compounds are well known to facilitate high rate and high voltage Li-ion batteries. Little is known, however, about spinel based electrodes for Na and Mg-ion batteries. Here we systematically study six spinel chemistries with first-principles statistical mechanics approaches to determine how the electrochemical properties of spinel compounds are affected by (i) host ionicity, (ii) guest cation radius, and (iii) guest cation oxidation state. As model systems, we consider spinel CoO_2 and TiS_2 as hosts and Li, Na, and Mg as guest cations. Electrochemical properties of spinel compounds are strongly dependent on guest cation site preferences. Our study shows that large guest cations prefer octahedral coordination, while the electrostatic interactions in ionic hosts favor tetrahedrally coordinated guest cations. The insights of this study suggest simple design principles with which new spinel intercalation compounds can be developed and indicate that transition metal oxide spinel compounds could enable high rate Na-ion batteries.

1 Introduction

Spinel intercalation compounds such as $LiMn_2O_4$ and $LiTi_2O_4$ exhibit exceptional rate capabilities when used as electrodes in Li-ion batteries.[1] The Mn based spinels are well suited as cathodes due to their high voltage[2–5] while the Ti derived spinels, with their substantially lower voltages, are more suited as anode materials.[6–9] The spinel crystal structure is also a promising intercalation host for Na and Mg-ion batteries. Recent experimental studies by Sun *et. al.* demonstrated that a sulfide spinel can intercalate Mg reversibly in a Mg-ion battery.[10] Manganese based spinel compounds have also shown promise as positive electrodes for Na-ion batteries.[11–13]

Spinel has a general chemical formula of AB_2X_4 and belongs to the $Fd\bar{3}m$ space group. The anions, X (i.e. oxygen or sulfur), of the spinel crystal structure occupy the 32e Wyckoff positions and form a face-centered cubic (FCC) lattice. The A cations occupy the 8a sites and are tetrahedrally coordinated by X, while the B cations occupy the octahedrally coordinated 16d sites. For instance, in spinels such as $LiMn_2O_4$, Li occupies the tetrahedral 8a sites and Mn occupies octahedral 16d sites.[2] The spinel crystal structure can also accommodate guest cations in the octahedrally coordinated 16c sites, which together with the tetrahedral 8a sites form a three-dimensional interconnected network that facilitates the rapid insertion and removal of guest cations[2] (see Fig. 1).

While a variation in the transition metal chemistry tends to affect the average voltage of the spinel compound,[14,15] much less is known about how anion chemistry (oxygen versus sulfur) and guest cation chemistry (Li versus Na versus Mg) affects the electrochemical properties of spinels. In transition metal oxide spinels, for example, Li prefers the tetrahedral sites, and only displaces to octahedral sites once the number of Li exceeds the number of available tetrahedral sites.[2,16] In a sulfide spinel such as TiS_2, in contrast, Li prefers the octahedral sites[17] at all compositions. Mg, which has the same ionic radius as Li but a higher valence, occupies tetrahedral sites in oxides such as $MgCr_2O_4$,[18] but prefers a mix of tetrahedral and octahedral sites in sulfide spinels such as TiS_2.[10,19] In spite of the increased interest in Na-ion batteries, very little is known about the behavior of Na in spinel compounds. The larger ionic radius of Na compared to those of Li and Mg suggests that different electrochemical properties should emerge upon insertion of Na into a spinel host.

Here we perform a first-principles statistical mechanics study of the electrochemical properties of spinel as a function of intercalating guest species and anion chemistry by focusing on six systems. We consider an oxide and a sulfide spinel, using spinel CoO_2 and TiS_2 as model host compounds. For each we determine the electrochemical properties, site preferences, and volume expansion upon insertion of Li, Na, and Mg. Li and Mg have the same ionic radius but a different valence, while Na has the same valence as Li but a larger ionic radius than both Li and Mg. This makes it possible to separate the role of ionic radius from ionic valence. The role of electrostatic interactions can be assessed by comparisons between the more ionic CoO_2 and the more covalent TiS_2 spinel hosts.

The results of this study reveal general principles with which to rationalize the electrochemical properties of spinels, which are to a large extent determined by guest cation site preferences. Guest cation radius plays an important role in determining site preference, with larger cations favoring octahedral sites. Electrostatic interactions, which become more important in oxide hosts, work in the opposite direction and favor tetrahedral occupancy. A higher guest cation oxidation state leads to an increased stability of cation-vacancy ordered phases and can lead to mixed occupancy over tetrahedral and octahedral sites. These principles can be combined to tailor the electrochemical properties of spinel intercalation compounds and suggest that Na insertion into oxide spinel hosts should enable high rate capable electrodes.

2 Methods

Density Functional Theory (DFT) as parametrized by Perdew Burke and Ernzerhoff (PBE)[20] was used to calculate formation energies of Li/Na/Mg-vacancy orderings over the interstitial sites of spinel CoO_2 and TiS_2. Projector augmented wave (PAW)[21,22] theory was used to approximate the core electrons. DFT calculations were performed using the Vienna ab-initio software package (VASP).[23,24] Plane-wave cutoff energies of 450, 530, and 600 eV were used for calculations containing Mg, Na, and Li respectively. A Monkhorst-Pack k-point grid of 7x7x7 was used for the primitive cell; calculations with larger supercells had a scaled grid to maintain or exceed the k-point density of the primitive cell. Formation energies of A-vacancy (A=Li,Na,Mg) configurations over the tetrahedral and octahedral sites of spinel CoO_2 and TiS_2 were used to train a cluster expansion Hamiltonian[25,26]

to predict the energy of arbitrary configurations within each spinel host. The cluster expansion Hamiltonians were used in grand canonical Monte Carlo simulations to calculate room temperature electrochemical properties, including open circuit voltage profiles and equilibrium site occupancies. The Clusters Approach to Statistical Mechanics (CASM) software package was used to construct and parametrize the cluster expansions and to perform the grand canonical Monte Carlo simulations.[27–30]

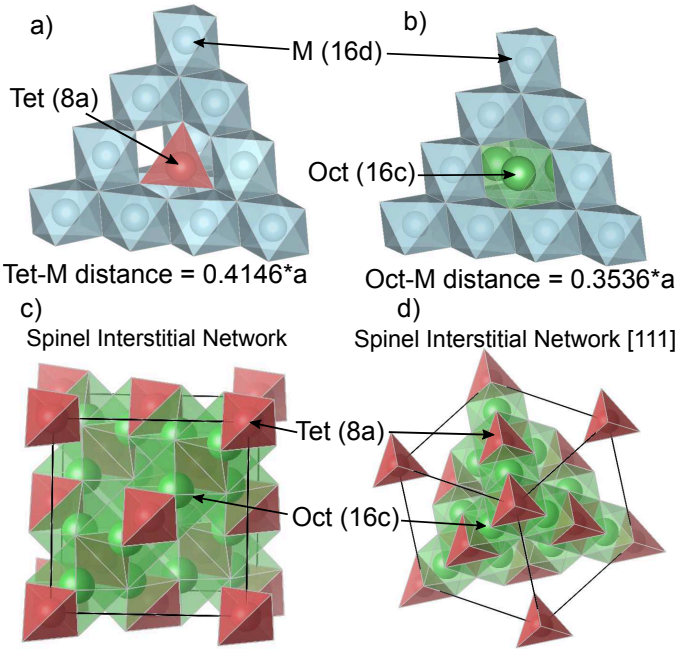

Figure 1: (a) The connectivity between a tetrahedral interstitial and the MX_2 framework of the spinel crystal structure. (b) The connectivity between octahedral interstitials and the MX_2 framework of the spinel crystal structure. (c) & (d) Intercalating species can fill a network of interconnected tetrahedral and octahedral sites within the spinel host. The tetrahedral (8a) sites form a diamond network with octahedral (16c) sites located between neighboring tetrahedral sites. The tetrahedral and octahedral sites share faces.

3 Results

Spinel intercalation compounds have cubic symmetry, with transition metal cations ordered over half the octahedral interstitial sites of a close-packed FCC anion sublattice. Li, Na, or Mg guest cations can occupy one of two distinct sets of interstitial sites that do not share faces with the transition metal containing octahedra. The tetrahedral (8a) sites form a diamond network, with each tetrahedral site surrounded by four octahedral (16c) sites. There are twice as many octahedral sites as tetrahedral sites, with each octahedral site sharing a face with two tetrahedral sites. Fig.

1 shows the connectivity of the MX_2 spinel framework and its interstitial sites. The simultaneous occupation of adjacent octahedral and tetrahedral sites is energetically unfavorable due to large electrostatic repulsions. Guest cation (i.e. Li, Na, or Mg) migration through the interstitial network of a spinel host requires elementary hops between adjacent octahedral and tetrahedral sites. A large difference in energy between the tetrahedral and octahedral sites will, therefore, result in high migration barriers for cation diffusion[16,17,31] and any strategy that equalizes the tetrahedral and octahedral site energies should lead to an enhancement of guest cation mobility within the spinel host.

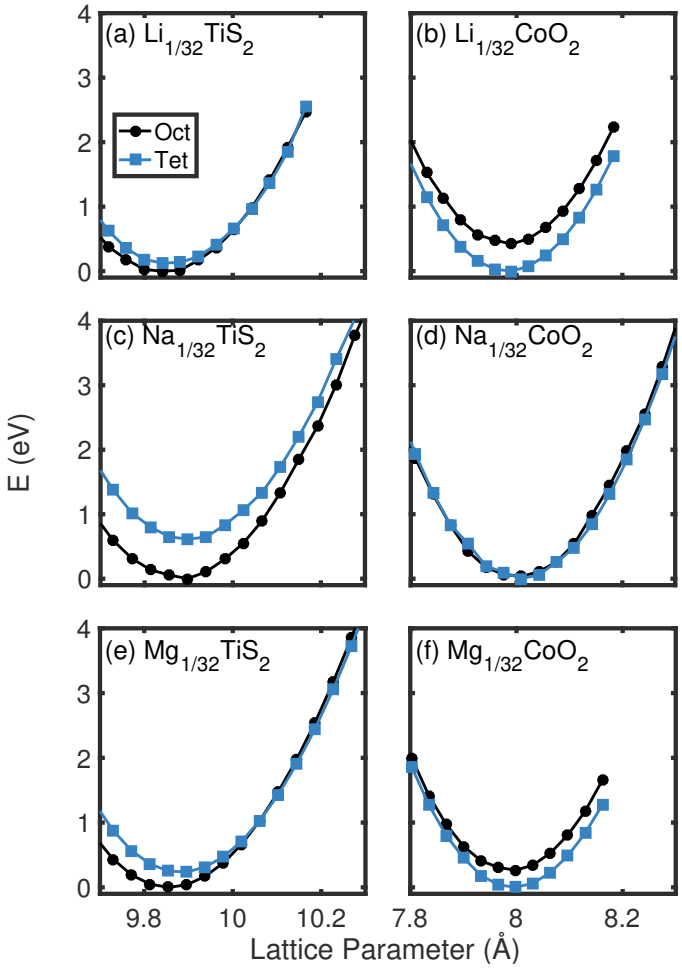

Figure 2: Total energies of octahedrally coordinated A-ions (black circle) and tetrahedrally coordinated A-ions (blue square) as a function of the conventional cubic cell lattice parameter of for the systems (a) Li_xTiS_2, (b) Li_xCoO_2, (c) Na_xTiS_2, (d) Na_xCoO_2, (e) Mg_xTiS_2, and (f) Mg_xCoO_2. Calculations were performed in the dilute limit in a cell that corresponds to a 2x2x2 supercell of the spinel primitive cell and a composition of $A_{1/32}MX_2$. The energy scale is relative to the lowest energy structure.

To identify the factors that determine site preference within spinel, we first calculated the relative

stability between octahedral 16c and tetrahedral 8a site occupancy in the dilute limit as a function of volume for Li, Na, and Mg in the TiS_2 and CoO_2 spinel hosts. Fig 2 shows the variation of the energy of an octahedral and a tetrahedral A-cation in a 2×2×2 super cell of the primitive spinel unit cell (i.e. $A_{1/32}MX_2$) as a function of the conventional cubic cell lattice parameter for the six systems. A comparison of Figs. 2 (a) and (e) and of Figs. 2 (b) and (f) shows that Li and Mg have very similar site preferences in both spinel TiS_2 and CoO_2 respectively. This is likely due to their similar ionic radii. In the sulfide spinel, both Li and Mg prefer the octahedral site at dilute concentrations, only marginally favoring the tetrahedral site at volumes that are substantially larger than the equilibrium volume of spinel TiS_2. In the oxide, the Li and Mg site preference is reversed, with both cations favoring the tetrahedral site over the octahedral site. This reversal can be attributed to the more ionic nature of the CoO_2 host compared to the more covalent TiS_2 host. The distance between the A-cation and its neighboring transition metal cations M in the 16d sites is larger for the tetrahedral 8a site than for the octahedral 16c site. The enhanced electrostatic interactions in the oxide, therefore, lead to a preference for tetrahedral 8a site occupancy as it enables an increased separation between positively charged cations.

A comparison between Li and Na intercalation in the CoO_2 and TiS_2 spinel hosts shows the importance of the cation radius in determining site preference. Fig.2 (c) shows that Na, with its larger ionic radius, prefers the octahedral site substantially more (by 0.3 eV to 1 eV) than the smaller tetrahedral site in TiS_2. In the more ionic $Na_{1/32}CoO_2$ oxide (Fig.2 (d)) the energies of the tetrahedral and octahedral sites are almost equal to each other (ranging between 0 and 150 meV). The enhanced electrostatic interactions that generally favor tetrahedral occupancy in the oxide is not sufficient to overcome the energetic cost of squeezing the larger Na cation into the smaller tetrahedral site, thereby making the tetrahedral and octahedral sites in CoO_2 essentially degenerate in energy at dilute Na concentrations.

Site preferences in spinel at higher guest cation concentrations can be revealed by considering formation energies of a large number of A-vacancy configurations within spinel TiS_2 and CoO_2 as a function of concentration. These are shown in Fig. 3. Configurations having only octahedrally (tetrahedrally) coordinated guest cations are shown in blue (red), while those having a mix of octahedral and tetrahedral occupancy are shown in purple. The majority of the ground state

configurations (the lowest energy configurations that reside on the convex hull) in TiS_2 contain octahedrally coordinated guest ions. Only in Mg_xTiS_2 are there ground state configurations at intermediate to high x that consist of a mix of octahedrally and tetrahedrally coordinated Mg ions. A comparison between the formation energies of Li_xTiS_2 and Na_xTiS_2 configurations shows that increasing the ionic radius of the guest cation while keeping its valence fixed, penalizes tetrahedral site occupancy in the spinel host. Fig. 3 (c) shows a very strong preference for octahedral occupancy at all concentrations in Na_xTiS_2, with configurations having any tetrahedral occupancy being substantially higher in energy compared to configurations having only octahedral occupancy.

Figs. 3 (b), (d), and (f) show a stronger preference for tetrahedral sites in the more ionic A_xCoO_2 spinel compounds. All Li_xCoO_2 ground states below $x = 1/2$ contain only tetrahedrally coordinated Li. Mg_xCoO_2 exhibits a similar trend, with the exception of the ground state at $x = 5/12$, which consists of a mix of tetrahedral and octahedral occupancy. While most Mg reside in tetrahedral sites in this ground state, some occupy octahedral sites, thereby increasing Mg-Mg pair distances. Both Li_xCoO_2 and Mg_xCoO_2 also exhibit a large two-phase region between $x = 1/2$ and $x = 1$ in which the guest cations transition from tetrahedral occupancy at $x = 1/2$ to octahedral occupancy at $x = 1$. The majority of ground state configurations in Na_xCoO_2, in contrast, have mixed tetrahedral and octahedral occupancy. Only at $x = 1/2$ do the Na cations exclusively occupy tetrahedral sites.

Intercalation of guest cations into a host compound is usually accompanied by a volume increase. Fig. 4 shows the cube root of the cell volume for A-vacancy configurations within spinel TiS_2 and CoO_2 that have energies within 10 meV/atom of the convex hull. The cube root of the volume can be used as a proxy for an averaged conventional cubic cell lattice parameter for each cation-vacancy configuration in spinel, even if the particular configuration does not strictly preserve cubic symmetry. While Fig. 4 shows that all compounds undergo a volume expansion with concentration, x, the Na_xCoO_2, Na_xTiS_2, Li_xCoO_2, and Mg_xCoO_2 systems exhibit very little variation in cell volume between configurations at each concentration. This is not true in Li_xTiS_2 and Mg_xTiS_2 which exhibit significant variations in cell volume at each concentration. Figures 4 (c) and (d) show that Na insertion into spinel induces larger volume changes of the host than that accompanying Li or Mg insertion.

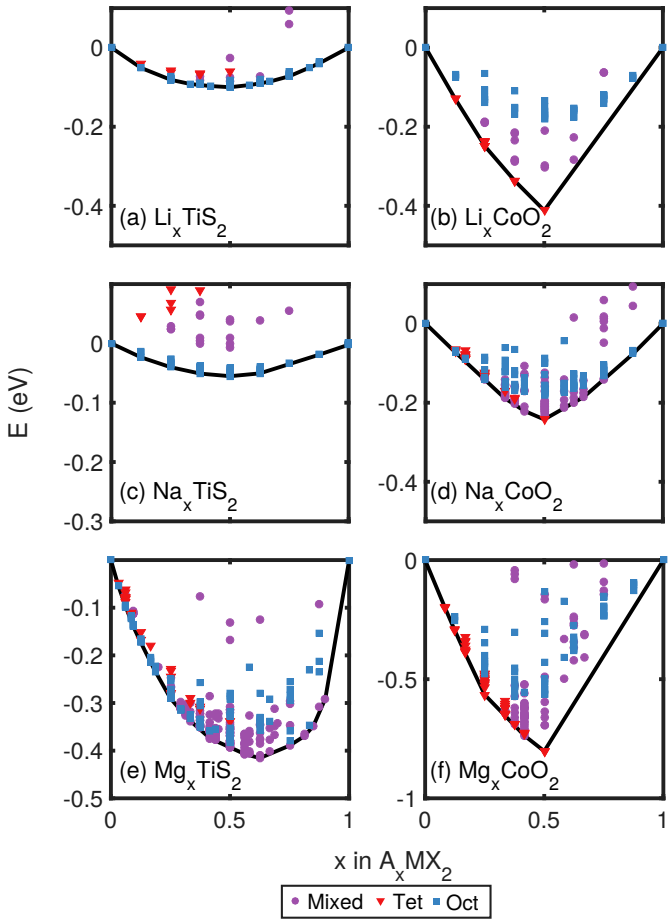

Figure 3: The formation energies (eV/formula unit) of A-vacancy configurations within spinel MX_2 as a function of A composition for the systems (a) Li_xTiS_2, (b) Li_xCoO_2, (c) Na_xTiS_2, (d) Na_xCoO_2, (e) Mg_xTiS_2, and (f) Mg_xCoO_2. Configurations that contain all octahedrally coordinated magnesium, all tetrahedrally coordinated magnesium, and mixed coordination correspond to blue squares, red triangles, and purple circles respectively. The convex hull (black line) connects the ground state configurations. Note that the scale on subfigure (c) and subfigure (f) are different due to a shallow and deep convex hull respectively.

The voltage of an electrode material is related to the chemical potential of the shuttled cation according to the Nernst equation

$$V(x) = -[\mu_{\mathrm{A}}(x) - \mu^{\circ}_{\mathrm{A}}]/ze \tag{1}$$

where z = 1 for Li and Na and z=2 for Mg. We calculated the chemical potentials of Li, Na, and Mg in spinel CoO_2 and TiS_2 at room temperature with grand canonical Monte Carlo simulations applied to cluster expansions of the configurational energy of cation-vacancy disorder. A separate

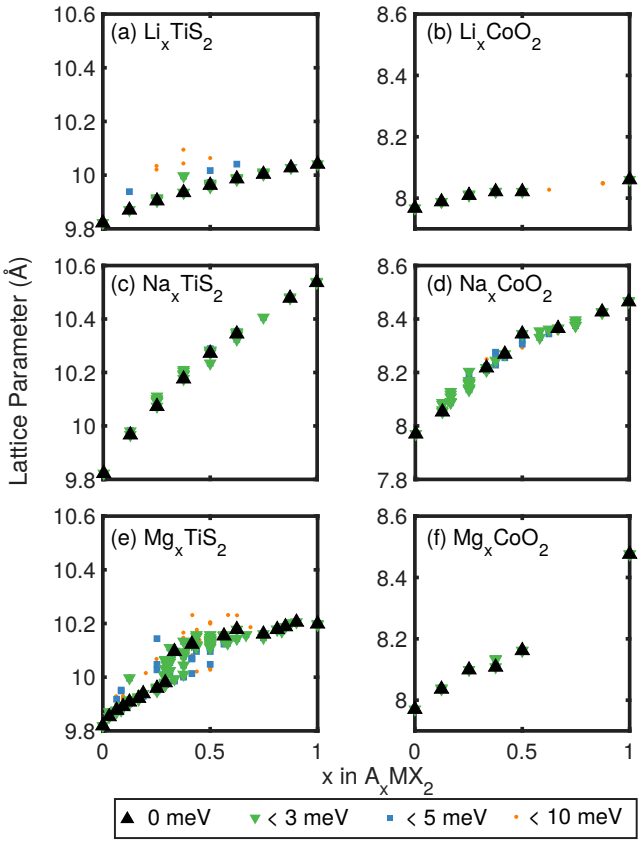

Figure 4: Cubic cell lattice parameter (calculated as the cube root of the cell volume) for spinel A_xMX_2 as a function of A composition at 0 K according to DFT for configurations with formation energies within 10 meV/atom from the convex hull for the systems (a) Li_xTiS_2, (b) Li_xCoO_2, (c) Na_xTiS_2, (d) Na_xCoO_2, (e) Mg_xTiS_2, and (f) Mg_xCoO_2. The black triangles, green triangles, blue squares, and orange circles represent the ground states, configurations with energies within 3 meV/atom, 5 mev/atom, and 10 meV/atom from the convex hull respectively.

cluster expansion was parameterized for each of the six spinel compounds using the DFT-PBE formation energies of Fig. 3 as training data.

Fig. 5 shows the calculated voltage profiles of all six compounds at room temperature (300 K). The sloping voltage profiles of the three sulfides indicate solid solution behavior. The voltage profiles of the oxide exhibit more pronounced features indicative of ordering reactions and phase transformations. The steps in the voltage profile indicate the occurrence of stable ordered phases at stoichiometric compositions while plateaus correspond to two-phase reactions. Both Li_xCoO_2 and Mg_xCoO_2 have voltage profiles that are qualitatively very similar. A large step at $x = 0.5$ separates a high voltage region between $x = 0$ and 0.5 from a plateau extending from $x = 0.5$ to 1 at lower voltages. While Na_xCoO_2 also exhibits a step at $x = 0.5$ it is not as large as in the Li and Mg

containing oxide spinels. Na_xCoO_2 also does not exhibit a large plateau between 0.5 and 1, but rather a smoother sloping profile signifying solid solution behavior toward the end of discharge.

More insight about the evolution of the voltage profiles can be gained by inspection of the site occupancy as a function of cation content. Fig. 6 shows the distribution of A cations on tetrahedral and octahedral interstitial sites as a function of composition. In Li_xTiS_2 and Na_xTiS_2, the cations exclusively occupy the octahedral sites. The Mg cations of Mg_xTiS_2 initially only fill octahedral sites but start to occupy a small fraction of tetrahedral sites as well beyond $x = 0.375$. All three sulfide spinels exhibit a solid solution at room temperature. The preference for octahedral sites in these compounds results in a sloping voltage profile.

Site occupancy in the oxides is more complex than in the sulfides. Li and Mg both prefer the tetrahedral sites over the octahedral sites in spinel CoO_2 below $x = 1/2$, although there is some mixed occupancy in Mg_xCoO_2 around $x = 5/12$ to maximize Mg-Mg pair distances. At $x = 0.5$ all tetrahedral sites are filled in Li_xCoO_2 and Mg_xCoO_2 and further increases in cation concentration must be accommodated by the less favorable octahedral sites. The filling of all tetrahedral sites results in a large step in the voltage profile at $x = 0.5$. Since the tetrahedral and octahedral sites share faces, the filling of octahedral sites requires a simultaneous displacement of tetrahedrally coordinated cations, which occurs through a two-phase reaction. This two-phase reaction manifests itself as a plateau between $x = 0.5$ and $x = 1$ in the voltage profile. Both Li_xCoO_2 and Mg_xCoO_2 also show smaller voltage steps below $x = 0.5$ due to cation ordering over the tetrahedral sites. In Na_xCoO_2, the tetrahedral and octahedral sites are essentially degenerate in energy. Hence Na insertion into spinel CoO_2 occurs on both tetrahedral and octahedral sites. At $x = 0.5$, the Na fill all tetrahedral sites as this configuration maximizes the distance between nearest neighbor Na cations at the 0.5 composition. Na_xCoO_2 also exhibits an extended solid solution beyond $x = 0.65$ consisting of mixed octahedral/tetrahedral occupancy. The voltage profile of Na_xCoO_2 is therefore, similar to those of the sulfides at low and high concentrations due to high octahedral site occupancy at those concentrations, but it also exhibits the large step that characterizes the voltage profiles of the other oxide spinels due to tetrahedral filling at $x = 0.5$.

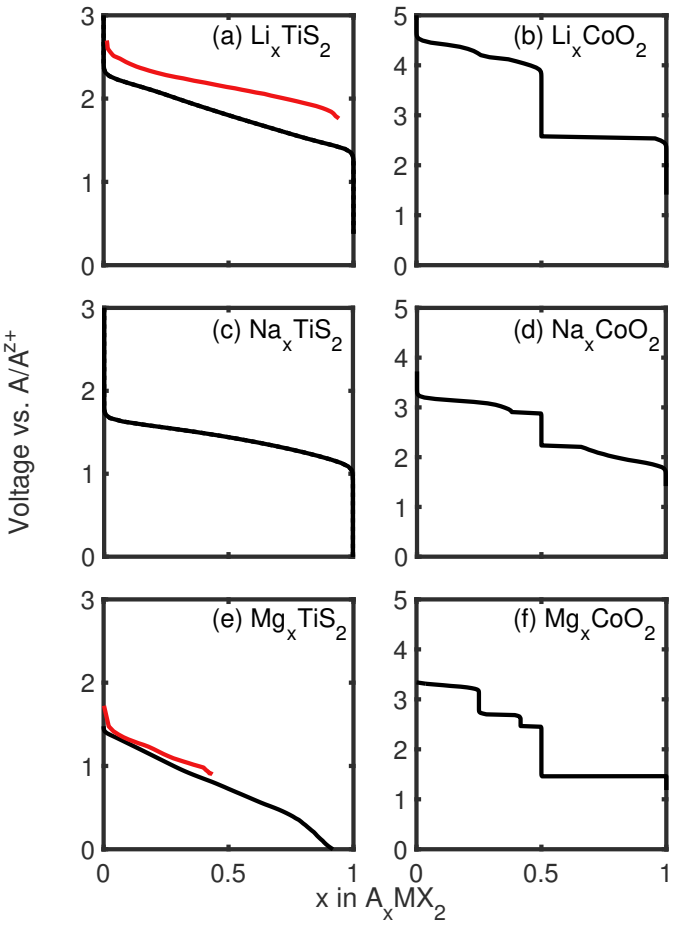

Figure 5: The calculated voltage of A_xMX_2 relative to A metal from a Monte Carlo simulation for the systems (a) Li_xTiS_2, (b) Li_xCoO_2, (c) Na_xTiS_2, (d) Na_xCoO_2, (e) Mg_xTiS_2, and (f) Mg_xCoO_2. An experimental voltage curve of Li_xTiS_2 / Li coin cell measured by Bonnick *et. al.* is shown on (a).[32] An experimental voltage curve of Mg_xTiS_2 / Mg coin cell measured by Sun *et. al.*[10] is shown on (e).

4 Discussion

Our first-principles statistical mechanics study of spinel A_xCoO_2 and A_xTiS_2 with A being either Li, Na or Mg has enabled a systematic determination of the effect of (i) host ionicity (i.e. oxide versus sulfide), (ii) the A cation radius and (iii) the A cation valence on the electrochemical properties of spinel intercalation compounds. Oxides are generally more ionic than sulfides. A clear manifestation of this emerges when comparing the A cation site preferences in spinel CoO_2 to those of TiS_2. Tetrahedral sites are preferred in more ionic spinel hosts, as it allows an increased separation between the postively charged guest cations and the transition metal cations. Furthermore, the tetrahedral 8a sites of spinel share corners with transition metal containing 16d octahedra, while

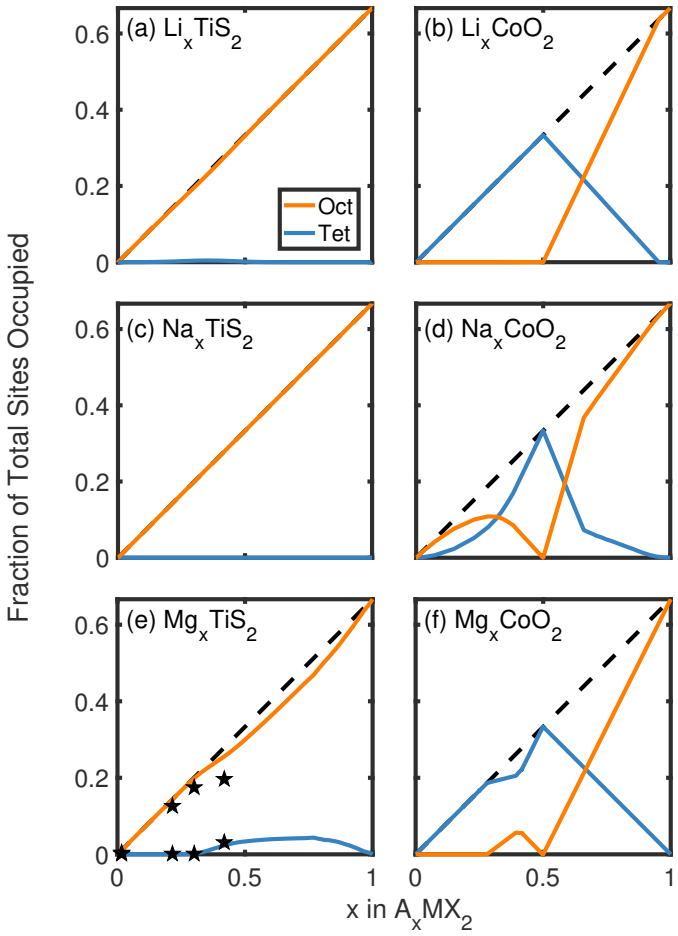

Figure 6: A concentration in the octahedral (orange line) and tetrahedral sites (blue line) of spinel at 333 K as calculated with Monte Carlo simulations for the systems (a) Li_xTiS_2, (b) Li_xCoO_2, (c) Na_xTiS_2, (d) Na_xCoO_2, (e) Mg_xTiS_2, and (f) Mg_xCoO_2. The black stars in (e) are experimentally measured concentrations from Sun *et. al.*[10]

the octahedral 16c sites share edges with the 16d sites (see Fig. 1). TiS_2 is a more covalent and compliant crystal than CoO_2, with the larger sulfur anion able to more effectively screen transition metal-intercalant electrostatic interactions. Octahedral sites are therefore preferred in TiS_2 as steric factors play a more important role.

The effect of guest cation radius on site preference in spinel is clearly revealed by the differences between the Li and Na containing spinels. The difference in energy between the smaller tetrahedral and the larger octahedral sites in spinel Na_xTiS_2 (between 0.3 eV and 1 eV) is significantly larger than in Li_xTiS_2 (between 0.1 eV and 0.5 eV), which can be attributed to the larger ionic radius of Na compared to that of Li. In the oxide spinel, where Li very much favors the tetrahedral sites, Na is more ambivalent, with tetrahedral and octahedral site energies being essentially degenerate.

The guest cation's formal oxidation state also plays a role in affecting electrochemical properties. While Li and Mg insertion into the same spinel host generates voltage profiles that are qualitatively similar to each other, there are differences. These can be attributed to a difference in the Li and Mg oxidation state since Li^+ and Mg^{2+} have very similar ionic radii. The voltage profile of Mg_xCoO_2 has larger steps than that of Li_xCoO_2 (especially at $x = 0.25$), signifying an increased stability of cation-vacancy orderings that is likely driven by stronger electrostatic interactions in the former. The Mg containing spinels also exhibit mixed tetrahedral/octahedral occupancy that is likely also driven by electrostatic interactions, as mixed occupancy at intermediate concentrations enables an increased separation between Mg pairs.

Guest cation mobility ranks among the most important properties that require optimization for battery applications. Cation transport within the spinel host arises from successive hops between nearest neighbor tetrahedral and octahedral sites.[16,17,31] Any reduction in the energy difference between the tetrahedral and octahedral sites of spinel will, therefore, lead to an increase in cation mobility.[33] The general principles revealed by this study show that the energy difference between tetrahedral and octahedral site occupancy in spinel can be controlled by tuning guest cation radius and host bonding character. The combination that appears to equalize the tetrahedral and octahedral site energies most is Na insertion into an oxide spinel. Indeed, the calculations of this study predict that the tetrahedral and octahedral sites are nearly degenerate in spinel CoO_2 upon insertion of Na. The flattening of the energy landscape in Na_xCoO_2 arises from a competition between electrostatic interactions, which favor tetrahedral sites, and steric factors, which favor the larger octahedral sites. However, not all transition metal oxide hosts are likely to be equally effective. Experimental studies indicate that Na prefers the tetrahedral 8a sites upon insertion into spinel MnO_2 (i.e. λ-MnO_2)[11] and $Ni_{0.25}Mn_{0.75}O_2$.[12] Tetrahedral occupancy in the Mn and Ni based spinel hosts is likely driven by the more ionic nature of these compounds, where valence electrons tend to be more localized since they occupy anti-bonding e_g orbitals centered at the transition metal sites.[34,35] Even then, the larger ionic radius of Na compared to that of Li, should result in lower migration barriers for Na diffusion compared to those for Li diffusion in the same spinel host.

We expect that alloying strategies exist with which the degree of ionic bonding of the spinel host can be fine-tuned to maximize Na ion mobility within spinel. Other factors must, of course,

also be taken into consideration when searching for optimal transition metal chemistries, including a determination of whether the chemistry favors the spinel crystal structure and can be synthesized and whether it is resistant to common electrochemical or mechanical degradation mechanisms.[34]

5 Conclusion

We investigated the effects of anion chemistry (oxide/sulfide) and guest cation chemistry (Li/Na/Mg) on the electrochemical properties of spinel intercalation compounds. The electrochemical properties of spinel compounds are extremely sensitive to guest cation site preferences. Two factors play a dominant role in determining guest cation site preference within spinel: (i) the guest cation radius, with larger cations favoring octahedral sites and (ii) the bonding character of the host, with the more ionic oxides favoring tetrahedral site occupancy. Our study has revealed simple design principles with which new spinel compounds can be developed and has indicated that Na insertion into oxide spinel compounds shows promise for high rate capable batteries. The large ionic radius of Na favors octahedral coordination while the ionic host of an oxide favors tetrahedral coordination, resulting in a unique equalization of the tetrahedral and octahedral site energies in spinel Na_xCoO_2. The energy difference between tetrahedral and octahedral sites in spinel is directly correlated with cation mobility and any flattening of the energy landscape will result in enhanced cation mobilities. We expect that these insights will lead to the discovery of transition metal oxide chemistries that will form spinel hosts that can be synthesized and that simultaneously enable high Na-ion mobilities.

Acknowledgement

S. K. Kolli is grateful for helpful discussions with Dr. Maxwell D. Radin, Julija Vinckeviciute, and John G. Goiri. This material is based upon work supported by the National Science Foundation, Grant DMR- 1410242. We acknowledge support from the Center for Scientific Computing from the CNSI, MRL: an NSF MRSEC (DMR-1121053). This research used resources of the National Energy Research Scientific Computing Center, a DOE Office of Science User Facility supported by the Office of Science of the U.S. Department of Energy under Contract No. DE-AC02-05CH11231.

References

(1) Whittingham, M. S. Lithium Batteries and Cathode Materials. *Chem. Rev.* **2004**, *104*, 4271–4302.

(2) Thackeray, M.; David, W.; Bruce, P.; Goodenough, J. Lithium insertion into manganese spinels. *Materials Research Bulletin* **1983**, *18*, 461–472.

(3) Thackeray, M.; Johnson, P.; de Picciotto, L.; Bruce, P.; Goodenough, J. Electrochemical extraction of lithium from LiMn2O4. *Materials Research Bulletin* **1984**, *19*, 179–187.

(4) Thackeray, M. M. Manganese oxides for lithium batteries. *Progress in Solid State Chemistry* **1997**, *25*, 1–71.

(5) Tarascon, J. M.; Wang, E.; Shokoohi, F. K.; McKinnon, W. R.; Colson, S. The Spinel Phase of LiMn[sub 2]O[sub 4] as a Cathode in Secondary Lithium Cells. *Journal of The Electrochemical Society* **1991**, *138*, 2859.

(6) Ohzuku, T.; Ueda, A.; Yamamoto, N. Zero-Strain Insertion Material of Li[Li[sub 13]Ti[sub 53]]O[sub 4] for Rechargeable Lithium Cells. *Journal of The Electrochemical Society* **1995**, *142*, 1431.

(7) Yi, T.-F.; Jiang, L.-J.; Shu, J.; Yue, C.-B.; Zhu, R.-S.; Qiao, H.-B. Recent development and application of Li4Ti5O12 as anode material of lithium ion battery. *Journal of Physics and Chemistry of Solids* **2010**, *71*, 1236–1242.

(8) Prakash, A. S.; Manikandan, P.; Ramesha, K.; Sathiya, M.; Tarascon, J.-M.; Shukla, A. K. Solution-Combustion Synthesized Nanocrystalline Li ₄ Ti ₅ O ₁₂ As High-Rate Performance Li-Ion Battery Anode. *Chemistry of Materials* **2010**, *22*, 2857–2863.

(9) Zhao, B.; Ran, R.; Liu, M.; Shao, Z. A comprehensive review of Li4Ti5O12-based electrodes for lithium-ion batteries: The latest advancements and future perspectives. *Materials Science and Engineering: R: Reports* **2015**, *98*, 1–71.

(10) Sun, X.; Bonnick, P.; Duffort, V.; Liu, M.; Rong, Z.; Persson, K. A.; Ceder, G.; Nazar, L. F. A high capacity thiospinel cathode for Mg batteries. *Energy Environ. Sci.* **2016**, *9*, 2273–2277.

(11) Yabuuchi, N.; Yano, M.; Kuze, S.; Komaba, S. Electrochemical behavior and structural change of spinel-type Li[LixMn2x]O4 (x=0 and 0.2) in sodium cells. *Electrochimica Acta* **2012**, *82*, 296–301.

(12) Kim, J. R.; Amatucci, G. G. Structural and Electrochemical Investigation of Na ⁺ Insertion into High-Voltage Spinel Electrodes. *Chemistry of Materials* **2015**, *27*, 2546–2556.

(13) Tarascon, J.; Guyomard, D.; Wilkens, B.; Mc Kinnon, W.; Barboux, P. Chemical and electrochemical insertion of Na into the spinel λ-MnO2 phase. *Solid State Ionics* **1992**, *57*, 113–120.

(14) Fey, G. T.-K.; Lu, C.-Z.; Kumar, T. Preparation and electrochemical properties of high-voltage cathode materials, LiMyNi0.5yMn1.5O4 (M=Fe, Cu, Al, Mg; y=0.00.4). *Journal of Power Sources* **2003**, *115*, 332–345.

(15) Liu, M.; Rong, Z.; Malik, R.; Canepa, P.; Jain, A.; Ceder, G.; Persson, K. A. Spinel compounds as multivalent battery cathodes: a systematic evaluation based on ab initio calculations. *Energy & Environmental Science* **2015**, *8*, 964–974.

(16) Bhattacharya, J.; Van der Ven, A. Phase stability and nondilute Li diffusion in spinel Li 1 + x Ti 2 O 4. *Physical Review B* **2010**, *81*, 104304.

(17) Bhattacharya, J.; Van der Ven, A. First-principles study of competing mechanisms of nondilute Li diffusion in spinel Li x TiS 2. *Physical Review B* **2011**, *83*, 144302.

(18) Chen, T.; Sai Gautam, G.; Huang, W.; Ceder, G. First-Principles Study of the Voltage Profile and Mobility of Mg Intercalation in a Chromium Oxide Spinel. *Chemistry of Materials* **2018**, *30*, 153–162.

(19) Kolli, S. K.; Van der Ven, A. First-Principles Study of Spinel MgTiS ₂ as a Cathode Material. *Chemistry of Materials* **2018**, *30*, 2436–2442.

(20) Perdew, J. P.; Burke, K.; Ernzerhof, M. Generalized Gradient Approximation Made Simple. *Physical Review Letters* **1996**, *77*, 3865–3868.

(21) Blöchl, P. E. Projector augmented-wave method. *Physical Review B* **1994**, *50*, 17953–17979.

(22) Kresse, G.; Joubert, D. From ultrasoft pseudopotentials to the projector augmented-wave method. *Physical Review B* **1999**, *59*, 1758.

(23) Kresse, G.; Furthmüller, J. Efficient iterative schemes for ab initio total-energy calculations using a plane-wave basis set. *Physical Review B* **1996**, *54*, 11169–11186.

(24) Kresse, G.; Furthmüller, J. Efficiency of ab-initio total energy calculations for metals and semiconductors using a plane-wave basis set. *Computational Materials Science* **1996**, *6*, 15–50.

(25) Sanchez, J.; Ducastelle, F.; Gratias, D. Generalized cluster description of multicomponent systems. *Physica A: Statistical Mechanics and its Applications* **1984**, *128*, 334–350.

(26) DeFontaine, D. Cluster Approach to Order-Disorder Transformations in Alloys. *Solid State Physics* **1994**, *47*, 33–176.

(27) CASM Developers, CASM, v0.2.X. Available from https://github.com/prisms-center/CASMcode. *CASM, v0.2.X. Available from https://github.com/prisms-center/CASMcode.* **2018**,

(28) Thomas, J. C.; Van Der Ven, A. Finite-temperature properties of strongly anharmonic and mechanically unstable crystal phases from first principles. *Physical Review B* **2013**, *88*, 214111.

(29) Van der Ven, A.; Thomas, J.; Xu, Q.; Bhattacharya, J. Linking the electronic structure of solids to their thermodynamic and kinetic properties. *Mathematics and Computers in Simulation* **2010**, *80*, 1393–1410.

(30) Puchala, B.; Van der Ven, A. Thermodynamics of the Zr-O system from first-principles calculations. *Physical Review B* **2013**, *88*, 094108.

(31) Van der Ven, A.; Bhattacharya, J.; Belak, A. A. Understanding Li Diffusion in Li-Intercalation Compounds. *Accounts of Chemical Research* **2013**, *46*, 1216–1225.

(32) Bonnick, P.; Sun, X.; Lau, K.-C.; Liao, C.; Nazar, L. F. Monovalent versus Divalent Cation Diffusion in Thiospinel Ti ₂ S ₄. *The Journal of Physical Chemistry Letters* **2017**, *8*, 2253–2257.

(33) Emly, A.; Van der Ven, A. Mg Intercalation in Layered and Spinel Host Crystal Structures for Mg Batteries. *Inorganic Chemistry* **2015**, *54*, 4394–4402.

(34) Radin, M. D.; Hy, S.; Sina, M.; Fang, C.; Liu, H.; Vinckeviciute, J.; Zhang, M.; Whittingham, M. S.; Meng, Y. S.; Van der Ven, A. Narrowing the Gap between Theoretical and Practical Capacities in Li-Ion Layered Oxide Cathode Materials. *Advanced Energy Materials* **2017**, 1602888.

(35) Radin, M. D.; Van der Ven, A. Simulating Charge, Spin, and Orbital Ordering: Application to JahnTeller Distortions in Layered Transition-Metal Oxides. *Chemistry of Materials* **2018**, *30*, 607–618.